Available online at www.sciencedirect.com
ScienceDirect
Genomics 90 (2007) 680–689
GENOMICS
www.elsevier.com/locate/ygeno

Gene expression profiling in livers of mice after acute inhibition of β-oxidation

Feike R. van der Leij [a,b,1], Vincent W. Bloks [a,1], Aldo Grefhorst [a], Jildou Hoekstra [a], Albert Gerding [a], Krista Kooi [c], Frans Gerbens [c], Gerard te Meerman [c], Folkert Kuipers [a,*]

[a] *Center for Liver, Digestive, and Metabolic Diseases, Laboratory of Pediatrics, University Medical Center Groningen, University of Groningen, CMCV, Room Y2.145, Hanzeplein 1, 9713 GZ Groningen, The Netherlands*
[b] *Unit Life Sciences, Van Hall Larenstein and Noordelijke Hogeschool, University of Applied Sciences, Leeuwarden, The Netherlands*
[c] *Department of Medical Genetics, University Medical Center Groningen, University of Groningen, Hanzeplein 1, 9713 GZ Groningen, The Netherlands*

Received 14 May 2007; accepted 6 August 2007
Available online 22 October 2007

Abstract

Inborn errors of mitochondrial β-oxidation cause ectopic fat accumulation, particularly in the liver. Fatty liver is associated with insulin resistance and predisposes to hepatic fibrosis. The factors underlying the pathophysiological consequences of hepatic fat accumulation have remained poorly defined. Gene expression profiling in a model of acute fatty liver disease induced by blocking long-chain fatty acid β-oxidation was performed to study the early effects of steatosis on the transcriptome. Tetradecylglycidic acid (TDGA) was used to irreversibly inhibit carnitine palmitoyltransferase 1, a key enzyme in the control of mitochondrial β-oxidation. TDGA treatment induced massive microvesicular hepatic steatosis within a 12-h time frame in male C57BL6/J mice. Increased hepatic long-chain acyl-CoA content, particularly of C16:0, C16:1 and C18:1, was associated with profound effects on the transcriptome as revealed by unbiased gene expression profiling and quantitative real-time PCR. The results indicate drastic changes in the expression of genes encoding proteins involved in lipid, carbohydrate, and amino acid metabolism. Pathway analysis identified transcription factors and coregulators such as hepatocyte nuclear factor 4 (HNF4), peroxisome proliferator-activated receptor-α (PPAR-α), and PPAR gamma coactivator 1α (PGC-1α) as key players in these metabolic adaptations. Apoptotic and profibrotic responses were also affected. Surprisingly, a strong reduction in the expression of genes involved in hepatic bile salt metabolism and transport was observed. Therefore, this transcriptome analysis opens new avenues for research.

Keywords: Transcriptome; Transcriptomics; Long-chain fatty acids; Steatosis; Bile salt metabolism; Peroxisome proliferator-activated receptor; Carnitine palmitoyltransferase; Etomoxir

Introduction

Defects in mitochondrial β-oxidation are associated with hypoketotic hypoglycemia and the accumulation of fat in organs such as the heart and the liver. Ectopic fat accumulation has been implicated in the development of metabolic derangements occurring in insulin-resistant states. The mechanisms underlying this relationship have only been partly revealed. It is known that in the liver nuclear receptors like peroxisome proliferator-activated receptor-α (PPAR-α) and hepatocyte nuclear factor 4 (HNF4) play pivotal roles in the genomic responses on accumulated intermediates of LCFA(long-chain fatty acids) metabolism [1–5]. The use of transcriptome analysis ("transcriptomics") should reestablish their roles, even though transcriptome analysis is limited to the measurement of steady-state levels of mRNA and the mRNA levels of these receptors themselves could remain unchanged. Next to these established pathways, new avenues of research can be opened with unbiased gene expression profiling as a first step toward addressing potential metabolic implications that were previously unknown.

* Corresponding author. Fax: +31 50 3611746.
E-mail address: f.kuipers@med.umcg.nl (F. Kuipers).
[1] Contributed equally to this study.

0888-7543/$ - see front matter © 2007 Elsevier Inc. All rights reserved.
doi:10.1016/j.ygeno.2007.08.004

Carnitine palmitoyltransferase I (CPT-I) is a key enzyme in the regulation of the mitochondrial β-oxidation of long-chain fatty acids [6,7]. The enzyme resides in the outer mitochondrial membrane [8] and is naturally inhibited by malonyl-CoA [6], the product of the first reaction in de novo fatty acid biosynthesis. The consequences of CPT-I inhibition include the accumulation of LCFA derivatives such as triglycerides (TGs), which is considered one of the earliest events in the development of insulin resistance [5,9]. Control of hepatic fatty acid metabolism, which is strongly interrelated with hepatic carbohydrate metabolism, plays a central role in the maintenance of whole body energy metabolism, particularly during fasting [1,10]. Processes involved in fatty acid metabolism are subject to stringent (post)-transcriptional control. Early events that occur during the development of nonalcoholic fatty liver disease (NAFLD), a condition that generally predisposes to nonalcoholic steatohepatitis (NASH), are of crucial importance since at this stage deleterious consequences may still be reversible. Whereas "chronic" NASH has been studied at various levels, including the application of microarray analysis [11], information on acute effects of hepatic lipid accumulation on hepatic gene expression is limited. Recent work has yielded considerable insight into the molecular mechanisms underlying the hepatic gene responses induced by fasting, a condition associated with "physiological" and reversible hepatic steatosis due to release of excess fatty acids from adipose tissue [12],which appears to be governed largely by PPAR-α [1–3].

However, the genome-wide consequences of a rise in cytosolic LCFA and long-chain acyl-CoA (LCAC) as such are not known. Therefore, we performed gene expression profiling in a model of acute hepatic steatosis induced by blocking LCFA β-oxidation to gain insight at the level of the transcriptome. Tetradecylglycidic acid (TDGA) was applied in mice to irreversibly inhibit CPT1 [7]. The model is characterized by massive microvesicular hepatic steatosis within a 12-h time frame, accompanied by the accumulation of TGs and nonesterified fatty acids (NEFA) in plasma. [13]. Under these conditions, gluconeogenesis was found to be only slightly suppressed while hepatic glucose production remained unaffected. TDGA-induced inhibition of FA oxidation in perfused rat livers decreased the hepatic ATP/ADP ratio by about 20% [14]. These data indicate that TDGA treatment does not induce an acute energy crisis in hepatocytes.

We aimed to quantify the degree of LCAC accumulation and to relate this to hepatic gene expression profiles in mice. Unbiased profiling was performed through the application of oligomer microarrays, whereas the expression of a selected number of genes was measured by quantitative real-time PCR. This acute model of hepatic steatosis revealed concerted changes in the expression of genes of major pathways in energy metabolism and hepatic cell cycle control and emphasizes a role for transcription factors and coregulators, such as HNF4, PPAR-α, and PGC-1α as well as of IGF-1. Surprisingly, the results show strong inhibition of several genes involved in hepatic bile acid metabolism and transport.

Results and discussion

Long-chain acyl-CoA accumulation in the livers of TDGA-treated mice

Quantification of hepatic TG content (+560%) and oil red O staining for neutral lipids confirmed the massive hepatic steatosis in TDGA-treated mice [13]. As expected from the site of action of TDGA, LC-acyl-CoA esters accumulated in the livers of TDGA-treated mice (Fig. 1). LCAC profiling revealed significantly ($P<0.05$) higher levels of myristoyl- (C14:0), palmitoyl (C16:0), palmitoleoyl- (C16:1), and oleoyl- (C18:1) CoA esters in livers of TDGA-treated mice. The accumulation of oleoyl-CoA was the most prominent. A predominance of 18:1 acyl species was also found in the VLDL-triglyceride profile obtained in the same model [13]. The total hepatic LCAC increase was less than 2-fold between control (123±48 nmol LCAC/g liver) and TDGA-treated mice (212±48 nmol LCAC/g liver) ($P=0.006$). This moderate increase probably is a consequence of rapid incorporation of LCAC into triglycerides (control, 19.9±8.3 μmol/g liver, vs TDGA, 112.4±25.2 μmol/g liver). As described [13], the TDGA-treated mice were hypoglycemic compared to controls during the course of the experiment, probably reflecting the use of glucose as energy source instead of fatty acids.

Global analysis of hepatic gene expression

For microarray analysis, we used two linear statistical approaches which, when combined, revealed a robust set of differentially expressed genes that was partly confirmed by real-time PCR analysis (see below). Principal component (PC) analysis on the complete data set showed that the second PC was informative for the hybridizations [15] of test versus control samples (Fig. 2, loop1 and loop 2) whereas this second component did not apply to the two self–self experiments. Employing a threshold for the standard deviation exceeding two (SD>2) yielded 403 genes to be differentially expressed according to PC analysis.

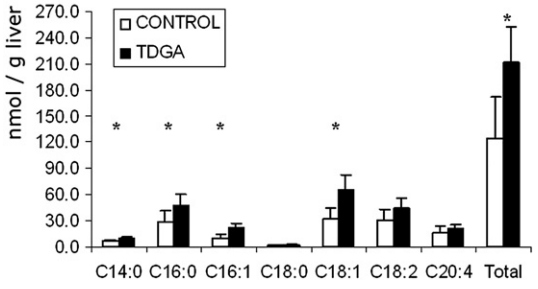

Fig. 1. Long-chain acyl-CoA profiles of livers from control and TDGA-treated mice.Tandem mass spectrometry after HPLC prepurification was used to obtain the LCAC profiles of livers from control (white bars, $n=5$) and TDGA-treated (black bars, $n=6$) mice. Asterisks denote significant ($P<0.05$) differences between specific chain-length LCAC species. All values represent means±SD for the number of animals indicated. Statistical analysis was carried out by applying the Mann Whitney U test.

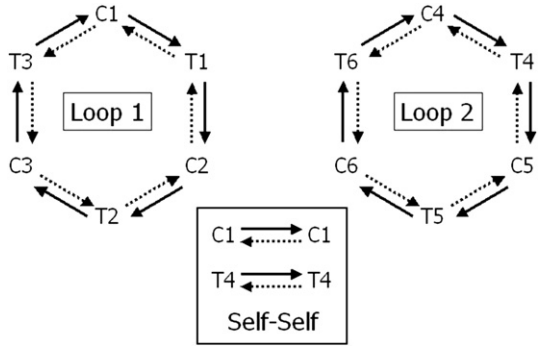

Fig. 2. Double loop model used in the microarray design. Two loops of hybridized cDNA from livers of control (C) and TDGA-treated (T) mice were applied, using 12 samples in total. The self–self hybridizations served as control experiments. Arrows indicate the direction of a hybridization: solid arrows symbolize green and dotted arrows red labeling of the cDNA.

The second statistical approach made use of array analysis according to the BRB software package from NIH. Raw data were filtered for reliability (allowing maximally 3 out of the 12 measurements per gene to be flagged or missing), which yielded 3226 genes. Of these genes, 411 were differentially expressed according to the criterion $P<0.001$.

The two sets of genes thus obtained had 232 differentially expressed genes in common, 52 of which were more than 2-fold higher expressed and 29 were more than 2-fold lower expressed in TDGA-treated animals compared to control animals. The full list of differentially expressed genes is added as Supplemental Table 2.

Real-time PCR

We measured the hepatic expression levels of 44 genes selected on the basis of reported function, by quantitative real-time PCR. Supplemental Table 1 lists all previously unpublished primers and probes used for real-time PCR. A list of the "fold change" values of the 44 genes determined by real-time PCR can be found in Supplemental Table 3. From the total of 232 differentially expressed genes identified by microarray as described above, 17 were tested for their expression level by real-time PCR. With the exception of one (the *Pygl* gene encoding glycogen phosphorylase), differential expression of all these genes was confirmed by real-time PCR. The direction of change and the "fold change" of these genes was comparable between microarray and real-time PCR (Fig. 3).

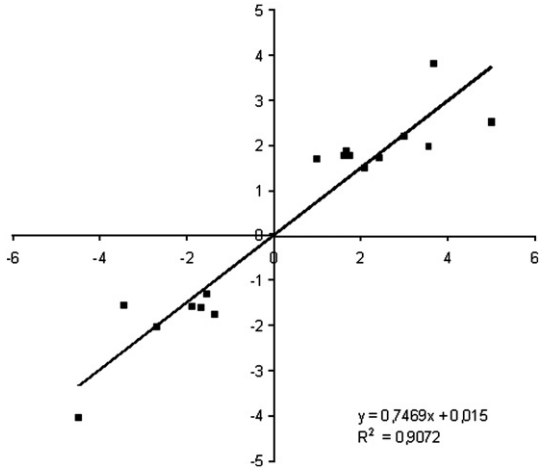

Fig. 3. Correlation of expression data from microarray and real-time PCR analysis. The "fold change" differences in expression levels as determined by microarray hybridizations (x-axis) and real-time PCR (y-axis) are plotted to visualize the quantitative correlation ($n=17$). These 17 genes are all in the set of 232 as obtained by microarray and that were measured by real-time PCR.

In addition, we determined the expression of several genes that did not show up in the microarray experiments. These genes were not represented on the chip (e.g., *Acaca*; *Cpt1b*), not in the filtered list of 3226 genes (e.g., *Acacb*), or showed P values higher than 0.001 in the microarray analysis (e.g., *Cpt1a*; *Pdk4*; *Cyp8b1*; *Cyp7a1*). However, these genes encode proteins that are considered of importance in hepatic lipid, carbohydrate, and bile acid metabolism and are intensively studied in our laboratory.

Table 1
Differentially expressed genes for transcription factors

Symbol	GenBank accession	Full gene name	Fold change	
			MA	PCR
Cbfa2t3h	NM_009824	Core-binding factor, runt domain, alpha subunit 2, translocated to, 3 homolog	3.66	
Bcl11a	NM_016707	B-cell CLL/lymphoma 11A (zinc finger protein)	2.84	
Ppargc1a	NM_008904	Peroxisome proliferative-activated receptor, gamma, coactivator 1 alpha	1.73	2.43
Mbd1	NM_013594	Methyl-CpG binding domain protein 1	2.1	
Peg3	NM_008817	Paternally expressed 3	1.94	
Nr1d1	NM_145434	Nuclear receptor subfamily 1, group D, member 1 (Reverb-a)		1.81
Sp3	AF062567	*trans*-acting transcription factor 3	1.8	
Nr1h3	AF085745	Nuclear receptor subfamily 1, group H, member 3 (LXR alpha)		−1.24
Esr1	NM_007956	Estrogen receptor 1 (alpha)	−1.41	
Nr1h4	NM_009108	Nuclear receptor subfamily 1, group H, member 4 (FXR)	−1.42	−1.52
Xbp1	NM_013842	X-box binding protein 1	−1.45	
Isgf3g	NM_008394	Interferon-dependent positive acting transcription factor 3 gamma	−1.94	
Stat2	NM_019963	Signal transducer and activator of transcription 2	−1.99	
Pou3f2	NM_008899	POU domain, class 3, transcription factor 2	−2.13	
Zfp35	NM_011755	Zinc finger protein 35	−2.29	
Bcl3	AF067774	B-cell leukemia/lymphoma 3	−2.58	
Srebf1	NM_011480	Sterol regulatory element binding factor 1		−2.62
Mlxipl	NM_021455	Williams-Beuren syndrome chromosome region 14 homolog (ChRebp)	−1.55	−3.44
Nr0b2	L76567	Nuclear receptor subfamily 0, group B, member 2 (SHP)		−4.49

The set of 232 genes obtained from microarray selection was increased by the differentially expressed genes according to real-time PCR to 250 genes. This set was used to create network representations. Global gene ontology analysis on the unbiased group of 232 genes indicated that most of the affected genes related to primary metabolic processes (Supplemental Table 4). For further interpretation we divided the differentially expressed genes into ontologically related subsets (Tables 1–6). The major subsets of differentially expressed genes are related to mitochondrial (Table 2) and peroxisomal (Table 3) functions including genes involved in lipid metabolism (Fig. 4), carbohydrate metabolism (Table 4), amino acid metabolism (Table 5), bile acid metabolism (Fig. 5), and apoptosis (Table 6). Transcription factors, central players in these processes, are listed in (Table 1). Surprisingly, no distinct subset of genes related to inflammation appeared to be induced in this acute model of hepatic steatosis. Likewise, no indications for macrophage infiltrations were evident from microscopical examination of liver sections. This is in contrast to high-fat diet-induced hepatic steatosis in mice, in which

Table 2
Differentially expressed genes for mitochondrial proteins

Symbol	GenBank accession	Full gene name	Fold change	
			MA	PCR
Pdk4	NM_053551	Pyruvate dehydrogenase kinase, isoenzyme 4		29.11
Cpt1b	NM_013200	Carnitine palmitoyltransferase 1b		7.29
Ucp3	NM_009464	Uncoupling protein 3, mitochondrial	2.5	5.01
Aass	NM_013930	Aminoadipate-semialdehyde synthase	3.6	
Crat	NM_007760	Carnitine acetyltransferase	2.19	3.00
Gpd2	NM_010274	Glycerol phosphate dehydrogenase 2, mitochondrial	2.38	
Grpel2	AF041060	GrpE-like 2, mitochondrial	2.17	
Acadm	NM_007382	Acetyl-coenzyme A dehydrogenase, medium chain		1.91
Acadl	NM_007381	Acetyl-coenzyme A dehydrogenase, long-chain		1.7
Gpam	NM_008149	Glycerol-3-phosphate acyltransferase, mitochondrial	1.88	1.69
Cpt2	NM_009949	Carnitine palmitoyltransferase 2		1.67
Fh1	U72679	Fumarate hydratase 1	1.66	
Ucp2	NM_011671	Uncoupling protein 2, mitochondrial	1.78	1.64
Slc25a20	NM_053965	Solute carrier family 25 (carnitine/acylcarnitine translocase), member 20		1.62
Slc25a15	NM_011017	Solute carrier family 25 (mitochondrial carrier ornithine transporter), member 15	1.58	
Amacr	NM_008537	Alpha-methylacyl-CoA racemase	1.55	
Cpt1a	NM_013495	Carnitine palmitoyltransferase 1a, liver		1.5
Glud1	NM_008133	Glutamate dehydrogenase 1	−1.35	
Sh3bp5	NM_011894	SH3-domain binding protein 5 (BTK-associated)	−1.49	
Nit2	AF284573	Nitrilase family, member 2	−1.51	
Cabc1	AJ278735	Chaperone, ABC1 activity of bc1 complex like (S. pombe)	−1.52	
Shmt1	NM_009171	Serine hydroxymethyl transferase 1 (soluble)	−1.55	
Sqrdl	NM_021507	Sulfide quinone reductase-like (yeast)	−1.65	
Pemt	NM_008819	Phosphatidylethanolamine *N*-methyltransferase	−1.36	−1.74
Hebp1	NM_013546	Heme binding protein 1	−1.8	
Hsb3b1	NM_008293	Hydroxy-delta-5-steroid dehydrogenase, 3-beta- and steroid delta-isomerase 1	−2.02	
Keg1	AB028071	Kidney expressed gene 1	−4.31	
Gck	L38990	Glucokinase	−4.04	−4.48

Table 3
Differentially expressed genes for peroxisomal proteins

Symbol	GenBank accession	Full gene name	Fold change	
			MA	PCR
Ehhadh	AJ011864	Enoyl-coenzyme A, hydratase/3-hydroxyacyl coenzyme A dehydrogenase	6.71	
Crat	NM_007760	Sarnitine acetyltransferase	2.19	3.00
Abcd3	NM_008991	ATP-binding cassette, sub-family D (ALD), member 3	1.98	
Peci	NM_011868	Peroxisomal delta3, delta2-enoyl-coenzyme A isomerase	1.77	
Pex19	Y09046	Peroxisomal farnesylated protein	1.64	
Amacr	NM_008537	Alpha-methylacyl-CoA racemase	1.55	
Pecr	AF232011	Peroxisomal *trans*-2-enoyl-CoA reductase	−1.49	
Hao1	NM_010403	Hydroxyacid oxidase 1, liver	−1.54	
Pipox	NM_008952	Pipecolic acid oxidase	−1.64	

Table 4
Differentially expressed genes for enzymes and transporters in carbohydrate metabolism

Symbol	GenBank accession	Full gene name	Fold change	
			MA	PCR
Pkm2	NM_011099	Pyruvate kinase, muscle	5.18	
Ppargc1a	NM_008904	Peroxisome proliferative-activated receptor, gamma, coactivator alpha	1.73	2.43
Gpd2	NM_010274	Glycerol phosphate dehydrogenase 2, mitochondrial	2.38	
Gfpt2	NM_013529	Glutamine fructose-6-phosphate transaminase 2	2.34	
Aldoa	NM_007438	Aldolase 1, A isoform, pseudogene 2	2.29	
Gys2	NM_145572	Glycogen synthase 2		1.8
G6pc	NM_008061	Glucose 6-phosphatase, catalytic	1.77	1.77
Fh1	U72679	Fumarate hydratase 1	1.66	
Hyal1	NM_008317	Hyaluronidase 1	−1.25	
Slc37a4	NM_008063	Solute carrier family 37 (glycerol-6-phosphate transporter), member 4	−1.52	
Gne	NM_015828	Glucosamine	−1.55	
Slc3a1	NM_009205	Solute carrier family 3, member 1	−1.63	
Khk	NM_008439	Ketohexokinase	−1.66	
PygI	AF288783	Liver glycogen phosphorylase	−1.69	
Slco1b2	NM_020495	Solute carrier organic anion transporter family, member 1b2 (oatp2)	−2.26	
B3galt1	NM_020283	UDP-Gal:betaGlcNAc beta 1,3-galactosyltransferase, polypeptide 1	−4.41	
Pklr	NM_013631	Pyruvate kinase liver and red blood cell		−4.43
Gck	L38990	Glucokinase	−4.04	−4.48

Table 5
Differentially expressed genes involved in amino acid metabolism[a]

Symbol	GenBank accession	Full gene name	Fold change	
			MA	PCR
Ehhadh	AJ011864	Enoyl-coenzyme A, hydratase/3-hydroxyacyl coenzyme A dehydrogenase	6.71	
Gfpt2	NM_013529	Glutamine fructose-6-phosphate transaminase 2	2.36	
Crat	NM_007760	Carnitine acetyltransferase	2.19	3.00
Aldh3a2	NM_007437	Aldehyde dehydrogenase family 3, subfamily A2	1.94	
Acadm	NM_007382	Acetyl-coenzyme A dehydrogenase, medium chain	1.91	
Adh7	NM_009626	Alcohol dehydrogenase 7 (class IV), mu or sigma polypeptide	1.72	
Glud1	NM_008133	Glutamate dehydrogenase	−1.35	
Pemt	NM_008819	Phosphatidylethanolamine *N*-methyltransferase	−1.36	−1.75
Akr1e1	NM_018859	Aldo-keto reductase family 1, member E1	−1.41	
Akr1c12	NM_013777	Aldo-keto reductase family 1, member C12	−1.44	
Shmt1	NM_009171	Serine hydroxymethyl transferase 1 (soluble)	−1.55	
Gclc	U85498	Glutamate-cysteine ligase, catalytic subunit	−1.59	
Pipox	NM_008952	Pipecolic acid oxidase	−1.64	
Gclm	NM_008129	Glutamate-cysteine ligase, modifier subunit	−1.82	
Got1	NM_010324	Glutamate oxaloacetate transaminase 1, soluble	−1.86	
Comt	NM_007744	Catechol-*O*-methyltransferase	−1.9	
Adh1	NM_007409	Alcohol dehydrogenase 1 (class I)	−2.13	
Cyp2a4	NM_009997	Cytochrome P450, family 2, subfamily a, polypeptide 4	−2.51	

[a] Note that some of these gene products are better known for their functions in other pathways (like fatty acid metabolism) but also act in steps of amino acid metabolic pathways.

rapid macrophage infiltration was recently reported to preced fat accumulation [16].

Insulin-sensitive genes are differentially expressed at the transcriptional level

Since hepatic insulin sensitivity appeared to be unaffected at the level of VLDL formation and phosphatidylinositol-3 kinase phosphorylation on TDGA treatment [13], we initially focused our attention on metabolic pathways that can be modulated by insulin. Several genes encoding proteins affected by insulin were found to be differentially expressed on TDGA treatment. The gene encoding SREBP-1c (sterol regulatory element binding protein-1c) was lower expressed in the livers of TDGA-treated mice compared to control (2.6-fold), whereas the *Pdk4* gene for pyruvate dehydrogenase kinase 4 and *Ppargc1a* (for PPAR gamma coactivator 1α; PGC-1α) were higher expressed (29.1- and 2.4-fold, respectively). These genes are all known to be highly insulin responsive: their strong regulation is compatible with a lowering of plasma insulin levels due to hypoglycemia on β-oxidation inhibition. Downstream targets of these proteins were switched off, e.g., *Gck*, *Pklr*, and *Pkm2* encoding glucokinase and liver- and muscle-type pyruvate kinase, respectively. Thus, genes involved in glycolysis were switched off and the key gene enabling inhibition of pyruvate oxidation (*Pdk4*) was switched on, probably reflecting responses aimed at sparing of glucose. In the condition of suppressed β-oxidation the body entirely depends on available glucose because neither ketone bodies nor energy needed for gluconeogenesis are being generated. The higher expression of *Ppargc1a* also known to occur during the fasting response could be a potential signal to increase gluconeogenesis [17,18]. *G6pc* (encoding the catalytic unit of glucose 6-phosphatase) was indeed higher expressed on treatment but expression of *G6pt* (*Slc37a4),* encoding the transporter subunit of glucose 6-phosphatase, was reduced and that of *Pck1* (*Pepck* for phosphoenol pyruvate carboxylase kinase) remained unaffected. The indifferent and low expression of the genes *Acaca* for acetyl-CoA carboxylase 1 and *Fasn* for fatty acid synthase, both involved in lipogenesis, is also compatible with low insulin levels, leading to suppressed SREBP-1c expression. These genes were already expressed at such low levels in the fasted control state that further down-regulation was not anticipated. Repression of the *Mlxipl* gene (3.45 times down) for the glucose-sensing transcription factor ChREBP (carbohydrate response element binding protein) is fully in line with impaired lipogenic gene transcription [19,20].

Genes involved in fatty acid oxidation are induced by a feedback mechanism

The massive changes in expression of genes encoding mitochondrial proteins may be part of a PGC-1α-mediated response. PGC-1α is the central orchestrating coactivator for mitochondriogenesis. Since mitochondria and peroxisomes are primary sites for oxidative processes it was not surprising to find many genes of fatty acid oxidation to be up-regulated.

Table 6
Differentially expressed apoptotic and antiapoptotic genes

Symbol	GenBank accession	Full gene name	Fold change	
			MA	PCR
Cidec	M61737	Fat-specific gene 27	5.68	
Tnfrsf12a	NM_013749	Tumor necrosis factor receptor superfamily, member 12a	4.31	
Cdkn1a	NM_007669	Cyclin-dependent kinase inhibitor 1A (P21)	2.53	
Sgk	NM_011361	Serum/glucocorticoid regulated kinase	1.77	
Btg2	NM_007570	B-cell translocation gene 2, antiproliferative	1.68	
Gadd45g	NM_011817	Growth arrest and DNA-damage-inducible 45 gamma	1.56	
Igf1	NM_010512	Insulin-like growth factor 1	−1.46	
Hsp90ab1	NM_008302	Heat shock protein 1, beta	−1.48	
Mcl1	NM_008562	Myeloid cell leukemia sequence 1	−1.48	
Cflar	NM_009805	CASP8 and FADD-like apoptosis regulator	−1.62	

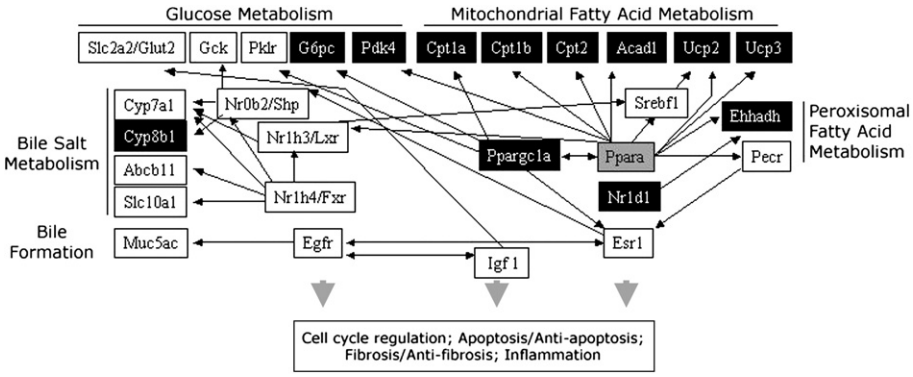

Fig. 4. Partial network representation. Several interconnected pathways were visualized by the use of the program Pathway Assist and Pathway Architect (Stratagene). A part of these networks is shown here, with black boxes for genes that are higher expressed, and white boxes for genes that were lower expressed in the livers of TDGA-treated mice. The gray box symbolizes unchanged expression of *Ppara*. The other gene symbols are explained in the text and tables.

Most of the genes involved are under the control of peroxisome proliferator-activated receptor α (PPAR-α, which is coactivated by PGC-1α). Since TDGA itself may act as a PPAR-α ligand [21], part of these effects may be a direct consequence of the treatment. These responses are characterized by overexpression of *Cpt1a* and *Cpt1b*, as well as other genes involved in β-oxidation *(Cpt2; Acadl; Acadm*) and LCFA partitioning (*Slc25a20; Ucp2; Ucp3*). The 5-fold increase in expression of the latter gene is in line with its proposed role as a mitochondrial fatty acid efflux protein [22]. Besides these feedback mechanisms, feed forward mechanisms may be involved as well. The response seems to anticipate a larger acetyl-CoA pool: the *Crat* gene encoding the buffering enzyme carnitine acetyltransferase was 3-fold higher expressed in the treated group. Carnitine acetyltransferase is important for both mitochondrial and peroxisomal acetyl-CoA and acetylcarnitine homeostasis [7]. Cellular carnitine uptake could be facilitated by the strong induction (almost 4-fold difference) of the gene encoding the plasma membrane carnitine transporter OCTN2. Many genes involved in the intracellular transport and the β-oxidation of LCFA are PPAR-α targets. Therefore, it is not surprising that PPAR-α is centrally positioned in a global pathway analysis such as depicted in Fig. 4.

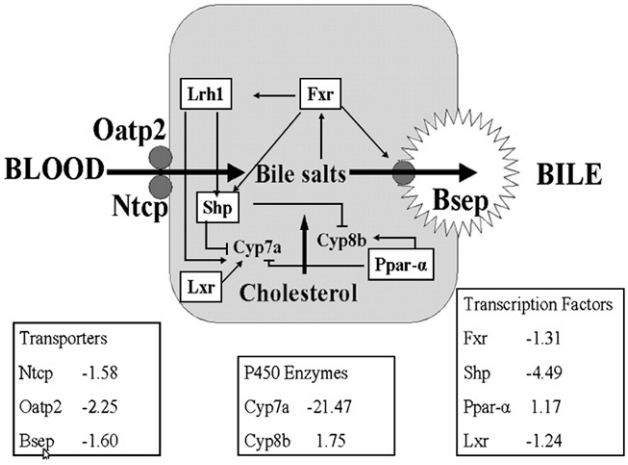

Fig. 5. Flawed expression of genes involved in bile salt metabolism. The liver cell with the bile canaliculus is schematically drawn, representing three major transporters in bile formation, i.e., the organic anion transporter 2 (Oatp2), Na^+/taurocholate cotransporter (Ntcp), bile salt exchange protein (Bsep), as well as two cytochrome P450 enzymes (Cyp7a and Cyp8b) and the trancription factors peroxisome proliferator-activated receptor-α (Ppar-α), liver X receptor (Lxr), short heterodimer partner (Shp), farnasoid X receptor (Fxr), and liver receptor homolog 1 (Lrh1). Positive actions are depicted by arrows, negative by blunted bars. Thick arrows indicate the flow of bile salts. Expression levels are indicated as "fold change" compared to control, as determined by real-time PCR. All changes shown were statistically significant according to the Mann Whitney *U* test, except Ppar-α.

Surprisingly, the *Acacb* gene for acetyl-CoA carboxylase 2 (ACC2) was 1.72-fold higher expressed in treated mice. This is remarkable since ACC2 is the isoform primary responsible for inhibition of CPT1 by malonyl-CoA in the liver [23]. Therefore, it was unexpected that this gene would become up-regulated in a situation of artificial inhibition of CPT1. The regulation of transcription of *Acacb* has not been elucidated [24] and our findings provide clues for further investigations.

In addition to PPAR-α as intracellular sensor of LCFA, it has been indicated that hepatocyte nuclear factor 4 is important in the concerted regulation of genes encoding the LCFA metabolic machinery. HNF4 is considered a master switch in the control of metabolic genes [4,5] and its importance in the development of diabetes is well-recognized [25]. As depicted in Supplemental Tables 2 and 3, 59 out of the 250 differentially expressed genes were associated with HNF4, accounting for 24% of total, indicating a major role of this nuclear receptor in the responses observed.

Circumstantial evidence suggests signaling by LCFA rather than LCAC

Blocking β-oxidation by TDGA results in hepatic accumulation of LCAC (Fig. 1). This accumulation was moderate compared to the profound effects on triglyceride accumulation. We found that the two genes encoding acyl-CoA synthases (*Acsl1* and *Slc27a4*) were more highly expressed in TDGA-treated mice than in controls (2.1- and 1.9 –fold, respectively). Both the *Acsl1* gene [26] and the *Slc27a4* gene for FATP4 [27] encode proteins that possess acyl-CoA synthetase activity. The latter contains a distinct peroxisome proliferator response element in its promoter [28]. The enzyme activities enable the

cell to covert LCFAs into their CoA esters which is needed for further partitioning.

When β-oxidation is blocked, LCFA are largely partitioned toward TG. The finding that the expression of two independent genes for acyl-CoA synthetases were induced provides circumstantial evidence, suggesting that the major effectors of the molecular cascades are the free LCFA rather than their CoA derivatives. Although acyl-CoAs are assumed to be important in the development of insulin resistance, the natural ligands of the nuclear receptors of the PPAR family and HNF4 are the free fatty acids rather than their CoA derivatives [3–5]. LCFA and LCAC accumulation can be detrimental due to the amphiphilic character of these molecules and, therefore, liver cells respond promptly by inducing the machinery to lower their concentrations. In addition, in nonliver tissue "futile cycling" has been proposed as an ATP-consuming mechanism through the action of fatty acid ligases and cytosolic thioesterase 1 (CTE1) [29]. Indeed, the gene for CTE1 was up-regulated 5-fold, suggesting that futile cycling is facilitated to occur in liver also. Alternatively, the hypoglycemia could be responsible for mobilization of fat resulting in high LCFA and elevated acyl-CoA synthase expression.

Triglyceride formation and proposed partial partitioning into VLDL

In the model studied, activation of LCFA could not be followed by β-oxidation and therefore the formation of TG in liver cells provided an immediate solution for avoiding intracellular LCFA and LCAC accumulation. Indeed, the *Dgat1* and *Gpam* genes that encode enzymes required for TG formation were induced on TDGA treatment, allowing the partitioning of LCAC into TG. *Dgat2* was lower expressed on the treatment, implying that the *Dgat1* over *Dgat2* ratio was increased. We reason that, despite the on-site accumulation of TG, a part of the TG is further partitioned into VLDL. As shown by Grefhorst et al. [13], total VLDL-TG production was not affected on TDGA treatment but analysis of particle composition revealed an enrichment with C18:1 acyl species coinciding with the composition of hepatic TG. Therefore, part of the accumulated TG must have been incorporated into nascent VLDL particles. *Apob* (1.25-fold up) is well known for its decisive role in VLDL formation by hepatocytes; yet, control is mainly exerted at posttranscriptional level [30,31]. The lower expression of *Pemt* is intriguing in this respect, since the *Pemt* gene product (phosphatidylethanolamine methyltransferase) is needed for the secretion of VLDL-apoB [32]. Interestingly, PEMT deficiency has recently been reported to aggravate hepatic steatosis in mouse models [33].

Bile salt metabolism is massively affected on the blocking of β-oxidation

An unexpected finding was the massive shift in expression of genes involved in bile salt metabolism and transport (Figs. 4 and 5). The *Cyp7a1* gene, encoding the rate-controlling enzyme in bile salts biosynthesis, was very strongly suppressed (21.5-fold) while *Cyp8b1,* which determines the cholate/chenodeoxycholate ratio, was 1.75-fold higher expressed. The transcriptional network including SHP (short heterodimer partner encoded by *Nr0b2*), LXR (liver X receptor encoded by *Nr1h3*), and FXR (farnesoid X receptor encoded by *Nr1h4*) as depicted in Figs. 4 and 5 may be involved in this regulation. PPAR-α is probably of prominent importance in this respect, as pharmacological PPAR-α activation leads to similar alterations in *Cyp7a1* and *Cyp8b1* gene expression in rodent livers [34,35].

It should be noted that the *Ehhadh* gene was drastically up-regulated (6.7-fold higher in TDGA-treated mice). This gene is of relevance for bile salt metabolism since its product enoyl-CoA hydratase/CoA dehydrogenase, also known as L-bifunctional protein, catalyzes the alternative pathway of peroxisomal side-chain shortening. However, its up-regulation may be primarily a consequence of PPAR-α-mediated gene transcription and can be regarded as part of the orchestrated up-regulation of the β-oxidation machinery rather than an increased need for side-chain shortening of bile salts. These results highlight an as yet unknown relationship between the transcription of genes needed for bile salt synthesis (i.e., cholesterol catabolism) and the accumulation of intermediates of fatty acid metabolism.

Insulin-like growth factor and other central players show reduced expression after blocking β-oxidation

For several pathways (Fig. 4), insulin-like growth factor 1 (IGF1) is a key regulatory protein. The gene encoding IGF1 was 1.46-fold underexpressed on TDGA treatment compared to control levels. In our analysis on pathway interconnections, IGF1 showed up as a primary site of regulation that results in changes in gene expression of major pathways of relevance for hepatic steatosis. A total of 10 genes known to be involved in apoptosis and antiapoptotic response were differentially expressed (Table 6). Two of the highly up-regulated genes are known to induce cell death (the *Cidec* gene was 5.68-fold and the *Tnfsf12* gene was 4.31-fold higher expressed). In addition, *Cyp4a10* known as marker for lipid peroxidation and responsive to PPAR-α [36], was 2.27-fold higher expressed on TDGA treatment. These responses are likely part of a process in the acute phase of steatosis development in which the liver cells have to find a new equilibrium between apoptotic and antiapoptotic activities. This is not surprising, given the fact that major consequences of blocking β-oxidation are related to mitochondria (Table 2) which have a central role in apoptotic cascades. Indeed, in a recent in vitro study employing liver slices, it was shown that blocking of LCFA β-oxidation may cause apoptosis, especially if the blockade is downstream of CPT1 [37]. However, in our study no signs of apoptosis or inflammation were observed, likely due to the short-term nature of the experiment.

Other effects that relate to lower expression of IGF1, and also of estrogen receptor1 (Erα, encoded by *Esr*) and epidermal growth factor receptor (EGFR) (Fig. 4), are the genes that control cell cycle (suppression of oncogenesis), as well as

fibrotic and antifibrotic responses (e.g., genes involved in collagen formation). These are obviously responses that are of relevance for the acute effects of hepatic steatosis and our data (added as Supplemental tables) may provide new angles to approach the molecular networks underlying these effects.

Comparison to other microarray studies

The number of studies applying high-throughput gene expression profiling in NAFLD is limited. These were carried out with livers from human subjects, which by definition reflect a more chronic state of steatosis. Compared to these studies, we observed a number of similarities. Apart from genes involved in fatty acid and carbohydrate metabolism as discussed above, we also encountered a large number of genes involved in amino acid metabolism (Table 5). Profound changes in energy metabolism are a plausible explanation for this finding, since many of the enzymes in amino acid metabolism are highly dependent on ATP and reducing equivalents. Part of these responses may be ascribed to PPAR-α activation [38].

Compared to the literature there are also important differences in outcome. For instance, responses to prevent oxygen damage and to induce scavenging were clear-cut in the study by Sreekumar et al. [11] but appeared not (yet) of relevance in our acute model. Another example refers to the fact that out of the list of 232 differentially expressed genes (Supplemental Table 2) we only found 3 genes encoding constituents of the cytoskeleton and 4 for extracellular matrix proteins whereas analysis of a large number of human subjects) indicated an important role for extracellular matrix remodeling [39,40].

Chiappini et al. [41] studied biopsies that did not show histological features of inflammation and therefore may be considered as intermediate acute phase samples. Indeed, in terms of classification (mitochondrial metabolism, inflammation) their findings most closely resemble the data presented here, although many detailed differences are apparent. The difference in composition of gene sets present on the microarrays may contribute to these differences.

Concluding remarks

It is important to note that it is not possible to discuss the relevance and impact of all genes and clusters that were differentially expressed in this study. Therefore, this initial analysis is focused on pathways that provide insight in the major responses that occur during the acute phase of steatosis development. By the use of transcriptome analysis we reestablished the roles of some important nuclear receptors, even though the use of primary data was limited to (sets of) genes that were differentially expressed without measuring gene product activity. Through pathway analysis the subsequently distilled information revealed important factors, even though the mRNA levels of these receptors themselves sometimes remained indifferent. Our results show also that gene expression profiling can be used as a first step toward addressing previously unknown implications, like altered expression of genes involved in bile salt metabolism and transport.

Materials and methods

Animals and chemicals

Male wild-type C57BL/6J mice (Harlan, Horst, the Netherlands) were housed and treated according to protocols approved by the Animal Experiments Ethical Committee of the University of Groningen. The mice were housed under 12-h light/12-h dark regime and were fed normal chow (RMH-B, Hope Farms, Woerden, the Netherlands) and water ad libitum, until experimentation. Tetradecylglycydic acid (TDGA), a kind gift from Dr. P.J. Voshol (LUMC, Leiden, the Netherlands), was suspended at a concentration of 2.0 mg/ml in a solution consisting of 90 mg/ml bovine serum albumin in saline.

Animal experiments

Mice received an i.p. injection with 30 mg TDGA per kg bodyweight ($n=6$) or vehicle ($n=6$ unless stated otherwise). Food was withdrawn but mice still had access to water. After 12 h, the mice were killed by cardiac puncture under isoflurane anesthesia. The abdomen was opened and the liver was quickly removed and immediately frozen in liquid nitrogen and stored.

Acyl-CoA profiling

Extraction of LCAC was performed in frozen liver tissue according to Mangino et al. [42] with slight modifications. Hepatic LCAC content was determined by tandem mass spectrometry after HPLC prepurification (HPLC-MS-MS) (Perkin Elmer/Biosystems Sciex; and Applied Biosystems). Multiple reaction monitoring was performed to measure the different long-chain acyl-CoA thioesters. The transitions used were the doubly charged *m/z* precursor ion of LCAC at Q1 and the *m/z* product ion of the adenine residue at Q3. Full protocols of these procedures are available on request.

Microarrays

The microarrays used contained the complete mouse oligonucleotide library version 1 (Sigma-Genosys/Compugen) printed in duplicate on UltraGAPS slides (Corning, Reading, UK). The mouse oligonucleotide library version 1 consists of 7524 gene-specific 65-mer oligos representing 7445 genes from a diverse range of functionalities. In addition, positive and negative controls were represented on the arrays. These microarrays were obtained from the Department of Anthropogenetics at the Radboud University, Nijmegen, the Netherlands, and are known to provide robust data [43].

RNA isolation and purification

Total RNA was isolated from 30 mg liver tissue by the use of Tri-Reagent (Sigma-Aldrich, Zwijndrecht, the Netherlands), according to the manufacturer's protocol. RNA was purified with a RNeasy min Elute Clean-up kit (Qiagen, Venlo, the Netherlands) according to the manufacturer's protocol. The integrity and concentration were determined on an Agilent Bioanalyser 2100 (Palo Alto, CA).

Probe construction, hybridization, and data acquisition

Labeling of cDNA molecules through incorporation of aminoallyl-labeled nucleotides was performed according to a protocol described at http://pga.tigr.org/sop/M004_1a.pdf. Briefly, for each RNA sample, first-strand amino-modified cDNA was synthesized by oligo(dT)-primed reverse transcription from 20 μg total RNA using Superscript II reverse transcriptase (Invitrogen, Paisly, UK) in the provided buffer and in the presence of 0.5 mM dATP, dCTP, dGTP, 0.3 mM dTTP, and 0.2 mM amino-allyl dUTP. After 16 h incubation at 42 °C the RT reaction was stopped and cDNA was purified as described. Purified

cDNA was fluorescently labeled with Cy3 or Cy5 fluorophores (Amersham Biosciences, Roosendaal, the Netherlands) as described previously [44]. Labeled cDNA was purified using Microcon YM-30 size-exclusion columns (Millipore, Amsterdam, the Netherlands).

Each probe was put together by mixing the labeled cDNA reactions from the appropriate samples together with 15 μg poly(dA) DNA (Qiagen, Hilden, Germany) and 7.5 μg human Cot-1 DNA (Invitrogen). This probe was heated at 95 °C for 3 min, cooled to 52 °C, and mixed with an equal volume of preheated (52 °C) hybridization buffer to a final concentration of 25% formamide, 5X SSC (saline sodium citrate) and 0.1% SDS. All hybridizations were performed under lifterslips (Erie Scientific, Portsmouth, UK) within hybridization chambers (Telechem, Sunnyvale) in a waterbath at 52 °C for 40 h. After hybridization the slides were washed, dried and scanned at 10 μm resolution in a GMS 428 laser scanner (Affymetrix, Santa Clara, CA). Image intensity data for each array feature was extracted by ImaGene 5.6 software (BioDiscoveries, Marina Del Rey, CA).

Microarray analysis and computation

A double loop design (Fig. 2) was applied to the microarray hybridization experiment to minimize the number of microarray slides and still include dye-swap readings for all samples [45]. In addition, a self–self hybridization was included for both the control and the treatment group to account for technical variation in the experiments. Expression analysis was performed by principal component analysis in SPSS (Chicago, IL) [15] and by gene expression analysis in the BRB-ArrayTools software package (BRB ArrayTools developed by Simon and Peng Lam. For this latter BRB ArrayTools analysis control spots were removed and raw array data were normalized for each printtip separately. Intensity data of oligomer spots considered as empty, bad, or negative were removed from the file and spots with more than 25% missing data across the experiment were not included in the analysis. Differentially expressed genes among the two classes were identified using a random-variance *t* test, an improvement over the standard separate *t* test as it permits sharing information among genes about within-class variation without assuming that all genes have the same variance [46]. Genes were considered statistically significant if their *P* value was less then 0.001. The datasets were compiled by the use of Genespring software. The most prominent gene ontologies were identified by DRAGON [47], Gostat [48], and DAVID [49]. Network presentations were created with Pathway Assist and Pathway Architect [50] (Iobion/Stratagene, Amsterdam, the Netherlands) for a primary setup, added with more detailed knowledge from the literature. The genes annotated for mitochondrial proteins and involvement in mitochondrial development were further curated according to the MiGene database [51]. A set of genes that appeared to be involved in amino acid metabolism was further identified by PathwayFinder/Pathway Miner [52].

PCR procedures

cDNA synthesis was performed using recombinant M-MLV reverse transcriptase (Sigma-Aldrich, Zwijdrecht, the Netherlands). Real-time quantitative PCR was performed as previously described [12]. Primers (Invitrogen, Paisly, UK) and fluorogenic probes (Eurogentec, Seraing, Belgium) used in these studies were described elsewhere (http://www.LabPediatricsrug.nl) or listed in Supplemental Table 1. All data were subsequently normalized to β-actin/18S rRNA ratio, which where analyzed in separate runs.

Acknowledgments

We kindly acknowledge Rolph Pfundt at Nijmegen University for providing the microarray slides and Fjodor van der Sluijs and Liu Yan (Pediatrics Dept., Groningen) for technical assistance. The work reported here was supported by the Netherlands Heart Foundation Grant 2001.081 (F.v.d.L.), the Netherlands Scientific Organization Grant 903-39-291 (F.K.) and Sigma Tau/Ethifarma (F.v.d.L.).

Appendix A. Supplementary data

Supplementary data associated with this article can be found, in the online version, at doi:10.1016/j.ygeno.2007.08.004.

References

[1] T.C. Leone, C.J. Weinheimer, D.P. Kelly, A critical role for the peroxisome proliferator-activated receptor alpha (PPARalpha) in the cellular fasting response: the PPARalpha-null mouse as a model of fatty acid oxidation disorders, Proc. Natl. Acad. Sci. U. S. A. 96 (1999) 7473–7478.
[2] S. Kersten, J. Seydoux, J.M. Peters, F.J. Gonzalez, B. Desvergne, W. Wahli, Peroxisome proliferator-activated receptor alpha mediates the adaptive response to fasting, J. Clin. Invest. 103 (1999) 1489–1498.
[3] J.D. Browning, J.D. Horton, Molecular mediators of hepatic steatosis and liver injury, J. Clin. Invest. 114 (2004) 147–152.
[4] G.B. Wisely, A.B. Miller, R.G. Davis, A.D. Thornquest Jr., R. Johnson, T. Spitzer, A. Sefler, B. Shearer, J.T. Moore, A.B. Miller, T.M. Willson, S.P. Williams, Hepatocyte nuclear factor 4 is a transcription factor that constitutively binds fatty acids, Structure 10 (2002) 1225–1234.
[5] S. Dhe-Paganon, K. Duda, M. Iwamoto, Y.I. Chi, S.E. Shoelson, Crystal structure of the HNF4 alpha ligand binding domain in complex with endogenous fatty acid ligand, J. Biol. Chem. 277 (2002) 37973–37976.
[6] J.D. McGarry, G.F. Leatherman, D.W. Foster, Carnitine palmitoyltransferase I. The site of inhibition of hepatic fatty acid oxidation by malonyl-CoA, J. Biol. Chem. 253 (1978) 4128–4136.
[7] R.R. Ramsay, R.D. Gandour, F.R. van der Leij, Molecular enzymology of carnitine transfer and transport, Biochim. Biophys. Acta 1546 (2001) 21–43.
[8] F.R. van der Leij, A.M. Kram, B. Bartelds, H. Roelofsen, G.B. Smid, J. Takens, V.A. Zammit, J.R. Kuipers, Cytological evidence that the C-terminus of carnitine palmitoyltransferase I is on the cytosolic face of the mitochondrial outer membrane, Biochem. J. 341 (Pt. 3) (1999) 777–784.
[9] J.D. McGarry, What if Minkowski had been ageusic? An alternative angle on diabetes, Science 258 (1992) 766–770.
[10] O.E. Owen, G.A. Reichard Jr., M.S. Patel, G. Boden, Energy metabolism in feasting and fasting, Adv. Exp. Med. Biol. 111 (1979) 169.
[11] R. Sreekumar, B. Rosado, D. Rasmussen, M. Charlton, Hepatic gene expression in histologically progressive nonalcoholic steatohepatitis, Hepatology 38 (2003) 244–251.
[12] T. Kok, H. Wolters, V.W. Bloks, R. Havinga, P.L. Jansen, B. Staels, F. Kuipers, Induction of hepatic ABC transporter expression is part of the PPARalpha-mediated fasting response in the mouse, Gastroenterology 124 (2003) 160–171.
[13] A. Grefhorst, J. Hoekstra, T.G. Derks, D.M. Ouwens, J.F. Baller, R. Havinga, L.M. Havekes, J.A. Romijn, F. Kuipers, Acute hepatic steatosis in mice by blocking beta-oxidation does not reduce insulin sensitivity of very-low-density lipoprotein production, Am. J. Physiol.: Gastrointest. Liver Physiol. 289 (2005) G592–G598.
[14] C. Gonzalez-Manchon, A. Martin-Requero, M.S. Ayuso, R. Parrilla, Role of endogenous fatty acids in the control of hepatic gluconeogenesis, Arch. Biochem. Biophys. 292 (1992) 95–101.
[15] A.P. Crijns, F. Gerbens, A.E. Plantinga, G.J. Meersma, S. de Jong, R.M. Hofstra, E.G. de Vries, A.G. van der Zee, G.H. de Bock, G.J. Te Meerman, A biological question and a balanced (orthogonal) design: the ingredients to efficiently analyze two-color microarrays with Confirmatory Factor Analysis, BMC Genomics 7 (2006) 232.
[16] R. Shiri-Sverdlov, K. Wouters, P.J. van Gorp, M.J. Gijbels, B. Noel, L. Buffat, B. Staels, N. Maeda, M. van Bilsen, M.H. Hofker, Early diet-induced non-alcoholic steatohepatitis in APOE2 knock-in mice and its prevention by fibrates, J. Hepatol. 44 (2006) 732–741.
[17] J.T. Rodgers, C. Lerin, W. Haas, S.P. Gygi, B.M. Spiegelman, P. Puigserver, Nutrient control of glucose homeostasis through a complex of PGC-1alpha and SIRT1, Nature 434 (2005) 113–118.

[18] P. Puigserver, Tissue-specific regulation of metabolic pathways through the transcriptional coactivator PGC1-alpha, Int. J. Obes. (Lond.) 29 (Suppl. 1) (2005) S5–S9.
[19] S. Ishii, K. Iizuka, B.C. Miller, K. Uyeda, Carbohydrate response element binding protein directly promotes lipogenic enzyme gene transcription, Proc. Natl. Acad. Sci. U. S. A. 101 (2004) 15597–15602.
[20] D. Letexier, O. Peroni, C. Pinteur, M. Beylot, In vivo expression of carbohydrate responsive element binding protein in lean and obese rats, Diabetes Metab. 31 (2005) 558–566.
[21] B.M. Forman, J. Chen, R.M. Evans, Hypolipidemic drugs, polyunsaturated fatty acids, and eicosanoids are ligands for peroxisome proliferator-activated receptors alpha and delta, Proc. Natl. Acad. Sci. U. S. A. 94 (1997) 4312–4317.
[22] P. Schrauwen, W.H. Saris, M.K. Hesselink, An alternative function for human uncoupling protein 3: protection of mitochondria against accumulation of nonesterified fatty acids inside the mitochondrial matrix, FASEB J. 15 (2001) 2497–2502.
[23] L. Abu-Elheiga, M.M. Matzuk, K.A. Abo-Hashema, S.J. Wakil, Continuous fatty acid oxidation and reduced fat storage in mice lacking acetyl-CoA carboxylase 2, Science 291 (2001) 2613–2616.
[24] S.Y. Oh, S.K. Park, J.W. Kim, Y.H. Ahn, S.W. Park, K.S. Kim, Acetyl-CoA carboxylase beta gene is regulated by sterol regulatory element-binding protein-1 in liver, J. Biol. Chem. 278 (2003) 28410–28417.
[25] D.T. Odom, N. Zizlsperger, D.B. Gordon, G.W. Bell, N.J. Rinaldi, H.L. Murray, T.L. Volkert, J. Schreiber, P.A. Rolfe, D.K. Gifford, E. Fraenkel, G.I. Bell, R.A. Young, Control of pancreas and liver gene expression by HNF transcription factors, Science 303 (2004) 1378–1381.
[26] D.G. Mashek, K.E. Bornfeldt, R.A. Coleman, J. Berger, D.A. Bernlohr, P. Black, C.C. DiRusso, S.A. Farber, W. Guo, N. Hashimoto, V. Khodiyar, F.A. Kuypers, L.J. Maltais, D.W. Nebert, A. Renieri, J.E. Schaffer, A. Stahl, P.A. Watkins, V. Vasiliou, T.T. Yamamoto, Revised nomenclature for the mammalian long-chain acyl-CoA synthetase gene family, J. Lipid Res. 45 (2004) 1958–1961.
[27] T. Herrmann, F. Buchkremer, I. Gosch, A.M. Hall, D.A. Bernlohr, W. Stremmel, Mouse fatty acid transport protein 4 (FATP4): characterization of the gene and functional assessment as a very long chain acyl-CoA synthetase, Gene 270 (2001) 31–40.
[28] B.I. Frohnert, T.Y. Hui, D.A. Bernlohr, Identification of a functional peroxisome proliferator-responsive element in the murine fatty acid transport protein gene, J. Biol. Chem. 274 (1999) 3970–3977.
[29] D.J. Durgan, J.K. Smith, M.A. Hotze, O. Egbejimi, K.D. Cuthbert, V.G. Zaha, J.R. Dyck, E.D. Abel, M.E. Young, Distinct transcriptional regulation of long-chain Acyl-CoA synthetase isoforms and cytosolic thioesterase 1 in the rodent heart by fatty acids and insulin, Am. J. Physiol.: Heart Circ. Physiol. (2006) H2480–H2497.
[30] N.O. Davidson, G.S. Shelness, Apolipoprotein B: mRNA editing, lipoprotein assembly, and presecretory degradation, Annu. Rev. Nutr. 20 (2000) 169–193.
[31] G.S. Shelness, J.A. Sellers, Very-low-density lipoprotein assembly and secretion, Curr. Opin. Lipidol. 12 (2001) 151–157.
[32] A.A. Noga, Y. Zhao, D.E. Vance, An unexpected requirement for phosphatidylethanolamine N-methyltransferase in the secretion of very low density lipoproteins, J. Biol. Chem. 277 (2002) 42358–42365.
[33] A.C. Igolnikov, R.M. Green, Mice heterozygous for the Mdr2 gene demonstrate decreased PEMT activity and diminished steatohepatitis on the MCD diet, J. Hepatol. 44 (2006) 586–592.
[34] D.W. Russell, The enzymes, regulation, and genetics of bile acid synthesis, Annu. Rev. Biochem. 72 (2003) 137–174.
[35] S.M. Post, H. Duez, P.P. Gervois, B. Staels, F. Kuipers, H.M. Princen, Fibrates suppress bile acid synthesis via peroxisome proliferator-activated receptor-alpha-mediated downregulation of cholesterol 7alpha-hydroxylase and sterol 27-hydroxylase expression, Arterioscler. Thromb. Vasc. Biol. 21 (2001) 1840–1845.
[36] X. Lin, Z. Chen, P. Yue, M.R. Averna, R.E. OstlundJr, M.A. Watson, G. Schonfeld, A targeted ApoB38.9 mutation in mice is associated with reduced hepatic cholesterol synthesis and enhanced lipid peroxidation, Am. J. Physiol.: Gastrointest. Liver Physiol. (2006) G1160–G1176.
[37] A.E. Vickers, P. Bentley, R.L. Fisher, Consequences of mitochondrial injury induced by pharmaceutical fatty acid oxidation inhibitors is characterized in human and rat liver slices, Toxicol. In Vitro (2006) 1173–1182.
[38] S. Kersten, S. Mandard, P. Escher, F.J. Gonzalez, S. Tafuri, B. Desvergne, W. Wahli, The peroxisome proliferator-activated receptor alpha regulates amino acid metabolism, FASEB J. 15 (2001) 971–978.
[39] A. Baranova, K. Schlauch, S. Gowder, R. Collantes, V. Chandhoke, Z.M. Younossi, Microarray technology in the study of obesity and non-alcoholic fatty liver disease, Liver Int. 25 (2005) 1091–1096.
[40] Z.M. Younossi, F. Gorreta, J.P. Ong, K. Schlauch, L.D. Giacco, H. Elariny, A. Van Meter, A. Younoszai, Z. Goodman, A. Baranova, A. Christensen, G. Grant, V. Chandhoke, Hepatic gene expression in patients with obesity-related non-alcoholic steatohepatitis, Liver Int. 25 (2005) 760–771.
[41] F. Chiappini, A. Barrier, R. Saffroy, M.C. Domart, N. Dagues, D. Azoulay, M. Sebagh, B. Franc, S. Chevalier, B. Debuire, S. Dudoit, A. Lemoine, Exploration of global gene expression in human liver steatosis by high-density oligonucleotide microarray, Lab. Invest. 86 (2006) 154–165.
[42] M.J. Mangino, J. Zografakis, M.K. Murphy, C.B. Anderson, Improved and simplified tissue extraction method for quantitating long-chain acyl-coenzyme A thioesters with picomolar detection using high-performance liquid chromatography, J. Chromatogr. 577 (1992) 157–162.
[43] M.A. van der Wiel, J.L. Costa, K. Smid, C.B. Oudejans, A.M. Bergman, G.A. Meijer, G.J. Peters, B. IJlstra, Expression microarray analysis and oligo array comparative genomic hybridization of acquired gemcitabine resistance in mouse colon reveals selection for chromosomal aberrations, Cancer Res. 65 (2005) 10208–10213.
[44] P.A.'t Hoen, F. de Kort, G.J. van Ommen, J.T. den Dunnen, Fluorescent labelling of cRNA for microarray applications, Nucleic Acids Res. 31 (2003) e20.
[45] M.K. Kerr, G.A. Churchill, Experimental design for gene expression microarrays, Biostatistics 2 (2001) 183–2101.
[46] G.W. Wright, R.M. Simon, A random variance model for detection of differential gene expression in small microarray experiments, Bioinformatics 19 (2003) 2448–2455.
[47] C.M. Bouton, J. Pevsner, DRAGON view: information visualization for annotated microarray data, Bioinformatics 18 (2002) 323–324.
[48] T. Beissbarth, T.P. Speed, GOstat: find statistically overrepresented gene ontologies within a group of genes, Bioinformatics 20 (2004) 1464–1465.
[49] G. Dennis Jr., B.T. Sherman, D.A. Hosack, J. Yang, W. Gao, H.C. Lane, R.A. Lempicki, DAVID: Database for annotation, visualization, and integrated discovery, Genome Biol. 4 (2003) 3.
[50] A. Nikitin, S. Egorov, N. Daraselia, I. Mazo, Pathway studio—The analysis and navigation of molecular networks, Bioinformatics 19 (2003) 2155–2157.
[51] S. Basu, E. Bremer, C. Zhou, D.F. Bogenhagen, MiGenes: a searchable interspecies database of mitochondrial proteins curated using gene ontology annotation, Bioinformatics 22 (2006) 485–492.
[52] R. Pandey, R.K. Guru, D.W. Mount, Pathway Miner: extracting gene association networks from molecular pathways for predicting the biological significance of gene expression microarray data, Bioinformatics 20 (2004) 2156–2158.